Research Square

Preprints are preliminary reports that have not undergone peer review.
They should not be considered conclusive, used to inform clinical practice,
or referenced by the media as validated information.

Generation and characterization of two induced pluripotent stem cell lines from a Saudi patient with skeletal dysplasia carrying the heterozygous COL2A1 variant NM_001844.5:c.1861G>A, p.(Gly621Arg), and two lines from his unaffected mother

Latifa Aljuid
King Abdulaziz University Faculty of Medicine
Maryam Alowaysi
KAIMRC: King Abdullah International Medical Research Center
Gustavo Ramirez
KAIMRC: King Abdullah International Medical Research Center
Moayad Baadheim
KAIMRC: King Abdullah International Medical Research Center
Mohammad Al-Shehri
KAIMRC: King Abdullah International Medical Research Center
Mohammad Abdullah Basabrain
King Abdulaziz University
Mustafa Daghistani
KAIMRC: King Abdullah International Medical Research Center
Heba Hashem
King Abdulaziz Medical City - Jeddah
Rwan Al Jahdali
King Abdulaziz Medical City - Jeddah
Hameedah AlBayjani
King Abdulaziz Medical City - Jeddah
Lujain Bahmeed
King Abdulaziz Medical City - Jeddah
Dina Alsururi
King Abdulaziz Medical City - Jeddah
Samerah Al Kathiri
King Abdulaziz Medical City - Jeddah
Dareen Al-Yousfi

King Abdulaziz University Faculty of Medicine

Ayman Elsamanoudy

King Abdulaziz University Faculty of Medicine

Manal Hosawi

KAIMRC: King Abdullah International Medical Research Center

Khaled Alsayegh

alsayeghkn@gmail.com

King Abdullah International Medical Research Center https://orcid.org/0000-0003-2654-835X

Research Article

Keywords: iPSC. COL2A1. Skeletal dysplasia. iMSC. Chondrogenic

Posted Date: November 25th, 2026

DOI: https://doi.org/10.21203/rs.3.rs-11777730/v1

License: This work is licensed under a Creative Commons Attribution 4.0 International License.
Read Full License

Abstract

Type II collagenopathies are a group of skeletal disorders caused by pathogenic variants in the *COL2A1* gene, which encodes type II collagen, a major component of the cartilage extracellular matrix. Understanding the mechanisms underlying these disorders remains challenging due to the limited availability of patient-derived cartilage tissue. Here, we generated two induced pluripotent stem cell (iPSC) lines from an 11-year-old male with skeletal dysplasia carrying a heterozygous *COL2A1* variant (NM_001844.5:c.1861G > A p.(Gly621Arg)), along with two lines from his unaffected mother, who served as a genetically related, non-isogenic control. All four lines maintained normal karyotypes, expressed pluripotency markers, and demonstrated the ability to differentiate into all three germ layers. All four lines gave rise to iMSC-like cells, although the efficiency of mesenchymal marker induction varied between clones, and these cells were subsequently subjected to chondrogenic pellet differentiation. Although differences in pellet morphology and Alcian Blue staining were observed between patient- and control-derived cultures, these qualitative findings alone do not establish impaired chondrogenesis. These patient-derived iPSC lines provide a human cellular model for further investigation of skeletal dysplasia associated with the *COL2A1* p.(Gly621Arg) variant.

Introduction

Skeletal dysplasias are a group of rare genetic disorders that affect bone and cartilage development, with an estimated combined prevalence of 1 in 5,000 live births [1]. Among these disorders, type II collagenopathies are caused by pathogenic variants in the *COL2A1* gene and are associated with a wide range of skeletal, ocular, auditory, and joint abnormalities [2]. The severity of these conditions varies from lethal skeletal abnormalities in newborns to milder forms that become apparent later in life [3]. Common clinical features include disproportionate short stature, delayed ossification, vertebral abnormalities, shortened limbs, and early-onset joint degeneration. Some patients also develop hearing loss and visual complications, which may further affect their mobility and quality of life [2].

The *COL2A1* gene encodes the α1 chain of type II collagen, one of the main structural components of the cartilage extracellular matrix (ECM). Type II collagen is essential for cartilage formation, skeletal growth, and endochondral ossification [4, 5]. It consists of three α1(II) chains that form a triple-helical structure, where glycine residues within the repeating Gly-X-Y sequence are important for proper collagen folding and stability [2]. Pathogenic variants in *COL2A1*, particularly those involving glycine substitutions, can interfere with collagen assembly and lead to protein misfolding, endoplasmic reticulum stress, and abnormal extracellular matrix formation [4, 6]. These changes can affect cartilage development and contribute to the skeletal abnormalities observed in affected patients. However, the effects of individual *COL2A1* variants on cartilage formation are still not fully understood.

Animal models have been used to study type II collagenopathies and have helped improve our understanding of the disease [6]. However, differences between human and animal skeletal development can limit their ability to reproduce the human disease phenotype [4, 6]. Studying cartilage directly from

affected patients is also difficult because cartilage tissue and viable chondrocytes are not easily accessible. Therefore, human cellular models are needed to better understand how *COL2A1* variants affect cartilage development.

Patient-derived iPSCs offer a useful approach for studying these disorders because they retain the patient's genetic background and can be differentiated into different cell types, including mesenchymal stem cells and chondrocytes [4, 7]. Previous studies have developed iPSC models carrying *COL2A1* variants, including p.(Arg989Cys), p.(Gly1113Cys), and p.(Arg719Cys), using CRISPR/Cas9 gene editing [8–10]. These studies have helped investigate how *COL2A1* variants affect chondrogenic differentiation and cartilage matrix formation. For example, an iPSC model carrying the p.(Arg719Cys) variant showed reduced extracellular matrix formation in iPSC-derived cartilage, resembling some features of the disease [11]. However, the effects of the _ NM_001844.5:c.1861G > A, p.(Gly621Arg) variant have not been extensively studied in human stem cell models. Establishing iPSC lines directly from an affected patient may help us better understand the effects of this variant in its original genetic background.

In this study, we generated and characterized two iPSC lines from a patient with skeletal dysplasia (SD) carrying the heterozygous *COL2A1* variant p.(Gly621Arg), along with two iPSC lines from his unaffected mother as a related control. The generated lines retained their respective genotypes, showed normal karyotypes, expressed pluripotency markers, and were able to differentiate into cells representing all three germ layers. We also examined their ability to differentiate into induced mesenchymal stem cells (iMSCs) and subsequently undergo chondrogenic differentiation. Both patient- and control-derived iPSCs gave rise to iMSC-like cells, which were subjected to chondrogenic pellet culture as a preliminary, qualitative assessment. These lines provide a genetically characterized resource for future studies of the effects of the *COL2A1* p.(Gly621Arg) variant on cartilage development.

Materials and Methods

Generation of Induced Pluripotent Stem Cells

Patient Recruitment and Ethical Approval

This study was approved by the Institutional Review Board (IRB) of the Ministry of National Guard Health Affairs, Jeddah, Saudi Arabia (Protocol No. NRJ22J/060/03), as part of the project “Establishing the Saudi National Platform of Stem Cells”. The study included an 11-year-old male carrying a heterozygous *COL2A1* mutation that causes an amino acid change from (Gly) to (Arg) at position 621(c.1861G > A, p.(Gly621Arg)). The study also included his unaffected 31-year-old mother who served as a non-isogenic control. Written informed consent was obtained from the patient's parent and from the healthy related donor before blood samples were collected for PBMC isolation and iPSC generation.

Peripheral Blood Mononuclear Cells (PBMCs) Isolation and Reprogramming

Peripheral blood (5–10 mL) was collected from the patient and his mother in EDTA tubes. PBMCs were isolated by density-gradient using Lymphoprep™ and SepMate™-50 tubes (STEMCELL Technologies, Cat. No. 07801) following the manufacturer's instructions. After centrifugation, the PBMCs were collected, washed with phosphate-buffered saline (PBS) containing 2% fetal bovine serum (FBS), and counted. For reprogramming, 7 × 10^5 PBMCs were electroporated with episomal reprogramming plasmids (pCE-hOCT4, pCE-hSK (SOX2 and KLF4), pCE-hUL (L-MYC and LIN28A), pCE-mP53DD, and pCXB-EBNA1) from the Epi5™ Episomal iPSC Reprogramming Kit (Thermo Fisher Scientific, Cat. No. A15960) using the Neon™ Transfection System (Thermo Fisher Scientific). The transfected cells were seeded onto Matrigel-coated dishes and cultured in Erythroid Expansion Medium (STEMCELL Technologies, Cat. No. 09860) for three days. Later, mTeSR™ Plus medium (STEMCELL Technologies) was introduced on day 4, followed by daily replacement of 50% of the medium. By day 10, the original medium had been fully replaced with mTeSR™ Plus. By days 21–25, colonies with embryonic stem cell–like morphology were manually picked and transferred to Geltrex™-coated 48-well plates containing mTeSR™ Plus medium. Established iPSC cultures were passaged with Versene solution at a 1:30 split ratio and maintained at 37°C in a humidified incubator with 5% CO_2 and 20% O_2.

Characterization of pluripotency and genomic integrity

Episomal Plasmid Screening

Established iPSC clones were screened for residual episomal reprogramming plasmids. Genomic DNA was extracted using the AllPrep DNA/RNA/Protein Mini Kit (Qiagen), following the manufacturer's instructions. Residual episomal vectors were detected by PCR using primers targeting the oriP/EBNA-1 region shared by the Epi5™ plasmids (Table 1). No EBNA-1 sequences were detected, consistent with clearance of the episomal reprogramming vectors from the iPSC clones at p10-13.

COL2A1 Variant PCR Verification

To confirm the presence of the disease-causing variant, the genomic region containing *COL2A1* NM_001844.5: c.1861G > A was amplified from extracted genomic DNA (P 10–13 and donor PBMCs) with primers spanning the variant site (Table 1). PCR was carried out using Phusion™ Green Hot Start II High-Fidelity PCR Master Mix (Thermo Fisher Scientific) at an annealing temperature of 65°C. Following purification, the PCR products underwent Sanger sequencing. The resulting chromatograms were compared with those of the original patient sample to confirm retention of the heterozygous *COL2A1* NM_001844.5:c.1861G > A, p.(Gly621Arg) variant in the established iPSC lines. The sequencing primer is listed in Table 1.

Short Tandem Repeat Analysis

Genomic DNA was extracted from all iPSC lines (p 10–13) and the corresponding PBMCs. Then, STR analysis was performed using the Applied Biosystems™ GlobalFiler™ PCR Amplification Kit, which

amplifies 24 loci (21 autosomal STR loci, DYS391, a Y-chromosome insertion/deletion marker and amelogenin). The amplified products were separated on a SeqStudio™ Genetic Analyzer (HID) and analyzed using GeneMapper™ ID-X Software.

Karyotype Analysis

For karyotype analysis, cells (P 13–21) were exposed to 0.3 µg/mL KaryoMAX™ Colcemid™ for 15 minutes before dissociation with TrypLE. The cells were then incubated in a hypotonic solution containing 75 mM potassium chloride for 20 minutes at 37°C and fixed in a 3:1 mixture of methanol and glacial acetic acid. A minimum of 20 metaphase spreads were examined.

Immunofluorescence

Cells were fixed in 4% paraformaldehyde for 15 minutes and washed with PBS. They were then permeabilized with PBS containing 0.1% Triton X-100 and blocked with PBS containing 1% gelatin for 45 minutes. The cells were incubated overnight at 4°C with primary antibodies against the selected markers. After washing, they were incubated with the appropriate secondary antibodies for one hour at room temperature (Table 1). Nuclei were counterstained with ProLong™ Gold Antifade Mountant with DAPI. Immunostaining images for pluripotency, trilineage and mesenchymal markers were acquired using an EVOS™ FL Auto 2 Imaging System (Thermo Fisher Scientific) equipped with Olympus 20× objectives. Pluripotency and trilineage immunofluorescence were performed at (p14–17).

Quantitative Reverse Transcription PCR (RT-qPCR)

Total RNA was isolated from the generated iPSC clones (p14–17), differentiated cells and iMSCs using the RNeasy Mini Kit (Qiagen, Cat. No. 74104) following the manufacturer's instructions. The RNA was then converted into complementary DNA (cDNA) with the High-Capacity cDNA Reverse Transcription Kit (Thermo Fisher Scientific, Cat. No. 4368813). Quantitative real-time PCR was carried out on the QuantStudio™ 7 Flex Real-Time PCR System using PowerSYBR™ Green Master Mix (Thermo Fisher Scientific, Cat. No. 4367659). Primers used for RT-PCR are listed in (Table 1). Relative gene expression was determined using the comparative Ct method. The Ct values of each target gene were normalized to the housekeeping gene *GAPDH* to calculate ΔCt, and fold changes in gene expression were calculated using the 2^−ΔΔCt method. The expression levels of pluripotency markers were compared with those of the H1 human embryonic stem cell (hESC) line, while trilineage differentiation markers were compared with the corresponding undifferentiated iPSCs. Expression of the iMSC markers is presented as relative expression normalized to GAPDH (2^−ΔCt).

In Vitro Trilineage Differentiation

The capacity of the generated iPSC clones to differentiate into all three embryonic germ layers was evaluated using the STEMdiff™ Trilineage Differentiation Kit (STEMCELL Technologies, Cat. No. 05230). Differentiation was started from iPSCs (p 14–17). Ectodermal, mesodermal, and endodermal differentiation was carried out following the manufacturer's instructions. Cells were seeded at the

recommended densities for each lineage and maintained in the respective differentiation media for the specified durations. Differentiation was then assessed by examining lineage-specific marker expression using RT-qPCR and Immunofluorescence. The antibodies and primers used for the differentiation are included in (Table 1).

Flow Cytometry Analysis for Pluripotency Markers

Flow cytometry was used to quantitatively assess the expression of selected intracellular markers. Cells were fixed and permeabilized using the BD IntraSure™ Kit (BD Biosciences, Cat. No. 641778). Following fixation of 4×10^5 cells (p 16–18) in reagent A for 10 minutes, cells were incubated with the appropriate primary antibodies diluted in reagent B for 30 minutes. Subsequently, the corresponding secondary antibodies were applied for 45 minutes (Table 1). Samples were analyzed using a BD FACSAria™ cell sorter. Marker-positive populations were determined by comparing stained samples with the appropriate secondary antibody-only stained controls.

Mycoplasma Detection

Mycoplasma contamination was assessed by end-point PCR using the Mycoplasma PCR Detection Kit (Abcam, Cat. No. ab289834) (p 16–18). Culture supernatants were collected from iPSC cultures that were at least 80% confluent and had not undergone a medium change for 48 hours. For each PCR reaction, 2.5 µL of supernatant was used. A positive control provided with the kit (500 bp) and a no-template negative control (water) were included in each run. PCR products were analyzed on agarose gel.

Induced Mesenchymal Stem Cells Differentiation

Established iPSCs (P 14–18) were differentiated into induced mesenchymal stem cells (iMSCs) using MSC growth medium consisting of high-glucose DMEM (Gibco) supplemented with 10% FBS, 1% NEAA, and 5 ng/mL bFGF. At passage 0, cells were transferred from 6-well plates into new 6-well plates at a 1:1 split ratio. Cells were maintained at 37°C with 5% CO_2, and the medium was changed every 2–3 days. After 7 days, the cells were dissociated using 0.25% Trypsin-EDTA and reseeded at passage 1 at a density of 5×10^5 cells per well in 6-well plates. On day 21, cells were collected for immunocytochemical staining and RT-qPCR analysis. The antibodies and primers used to assess mesenchymal markers are listed in Table 1.

Chondrogenic Differentiation and Validation

Chondrogenic differentiation of the generated iMSCs was performed using the MesenCult™-ACF Chondrogenic Differentiation Kit (STEMCELL Technologies, Cat. No. 05455), following the manufacturer's protocol. On day 0, 1.25×10^5 iMSCs were added to 15 mL conical tube. On day 3, fresh medium was added, and starting from day 6, the medium was changed every 2–3 days. Cells were

maintained under three-dimensional (3D) culture conditions for 21 days. On day 21, the resulting pellets were collected for Alcian Blue staining. One pellet was formed per tube, and 4 pellets were generated per line.

Alcian Blue Staining

Whole-pellet Alcian Blue staining was used to evaluate chondrogenic differentiation. Pellets were fixed in 4% paraformaldehyde for 10 minutes, rinsed with 0.1 N HCl, and stained for one hour with Alcian Blue solution at pH 1.0. The stained pellets were then washed with 0.1 N HCl until the wash solution was colourless, rinsed with ddH_2O, and imaged using bright-field microscopy at 4× magnification.

Statistical Analysis

Quantitative data were reported as mean ± standard deviation. Statistical significance was evaluated using tests appropriate to each experimental comparison. Gene expression data were compared using Student's t-test, with $p < = 0.05$ considered statistically significant.

Results

Clinical and Genetic Characterization

An 11-year-old male patient diagnosed with skeletal dysplasia was included in this study. The patient presented with severe short stature, delayed growth, underdeveloped limbs, frontal bossing, and a short neck. Whole-exome sequencing identified a heterozygous missense variant in the *COL2A1* gene (NM_001844.5: c.1861G > A, p.(Gly621Arg)), resulting in the exchange of glycine with arginine at position 621 (performed by the clinical Molecular Diagnostics laboratory). This change affects the triple-helical domain of type II collagen, where glycine residues are essential for maintaining the structural stability of the collagen triple helix [12–14]. The variant was reported as likely pathogenic in the patient's genetic testing report, based on the interpretation provided by CENTOGENE. This variant has previously been reported in ClinVar (Variation ID: 196112) and is classified as pathogenic or likely pathogenic [15]. Although the variant has been identified in previous clinical genetic testing, its association with skeletal dysplasia has not been extensively characterized in the published literature. Together, these genetic findings are consistent with the patient's clinical presentation of skeletal dysplasia. The study also included the patient's unaffected mother, who does not carry the variant and served as a related, non-isogenic control.

Derivation and Establishment of SD Patient- and Control-Derived iPSC Lines

PBMCs were isolated from an 11-year-old male patient and his unaffected mother, who served as the control. Electroporation of PBMCs was performed on the day of blood collection. Episomal vectors encoding OCT4, SOX2, KLF4, L-MYC, LIN28, mp53DD, and EBNA1 were introduced into the PBMCs by

electroporation (Fig. 1A). Several embryonic stem cell-like colonies emerged approximately 21–25 days after transfection. A total of four clonal lines were established, two from the SD patient and two from the healthy control. The colonies exhibited characteristic human pluripotent stem cell morphology, including compact growth, well-defined borders, tightly packed cells, and a high nucleus-to-cytoplasm ratio (Fig. 1B). Colonies displaying these features were manually picked, expanded under feeder-free conditions, and cryopreserved at the KAIMRC facility for subsequent characterization. All generated SD-iPSC lines from the patient (KAIMRCi008-A and KAIMRCi008-B) and his healthy mother (KAIMRCi009-A and KAIMRCi009-B) were tested for the presence of residual episomal vectors (p 10–13). The clones showed complete clearance of the reprogramming plasmids before further characterization (Figure S1A).

Karyotype analysis of both patient-derived lines (KAIMRCi008-A and KAIMRCi008-B) revealed a normal male karyotype (46,XY), while the control lines (KAIMRCi009-A and KAIMRCi009-B) showed a normal female karyotype (46,XX). No numerical or structural chromosomal abnormalities were detected in the metaphase spreads examined (p 13–21) (Fig. 1C). Sanger sequencing confirmed the presence of the heterozygous *COL2A1* variant (c.1861G > A, p.(Gly621Arg)) in the patient's peripheral blood cells and derived SD-iPSC lines, while the variant was absent in the healthy-control-derived lines (Fig. 1D). Short tandem repeat (STR) analysis was performed to verify donor identity and confirmed that the iPSC lines genetically matched their respective donor PBMCs. STR profiles were identical between each iPSC line and its donor PBMCs at all 20 autosomal STR loci, DYS391, a Y-chromosome insertion/deletion marker and amelogenin was reported (Figure S1B). Furthermore, routine screening confirmed that all generated iPSC lines were free of mycoplasma contamination by end-point PCR (Figure S1C).

Characterization of pluripotency of SD Patient- and Control-Derived iPSC Lines

The patient- and control-derived iPSC lines were assessed using molecular and cellular methods to verify successful reprogramming. Pluripotency was evaluated by flow cytometry, immunofluorescence, and RT-qPCR. Flow cytometry showed that most cells expressed the corresponding pluripotency markers. KAIMRCi008-A showed OCT4, NANOG, and SOX2 positivity in 99.0%, 98.5%, and 95.7% of cells, respectively. In KAIMRCi008-B, the corresponding proportions were 98.9%, 94.8%, and 99.3%. KAIMRCi009-A showed 98.3% OCT4-positive, 91.1% NANOG-positive, and 98.2% SOX2-positive cells; the respective values for KAIMRCi009-B were 96.9%, 98.7%, and 98.5% (Fig. 2A). Immunofluorescence also confirmed OCT4, SOX2, and NANOG expression in both patient- and control-derived iPSC lines (Fig. 2B). RT-qPCR confirmed expression of the pluripotency-associated genes *OCT4*, *SOX2, and NANOG* in all established iPSC clones, using H1 human embryonic stem cells (hESCs) as the reference (Fig. 2C).

The differentiation potential of the established iPSC lines was examined by directed differentiation into the three germ layers, accompanied by assessment of lineage-associated gene expression. Ectodermal differentiation was associated with *NESTIN* and *PAX6* expression, mesodermal differentiation with *TBXT* (*BRACHYURY*) and *CDX2* expression, and endodermal differentiation with *SOX17* and *GATA4* expression

(Fig. 3A) (log2 fold change relative to the corresponding undifferentiated iPSCs). Immunofluorescence staining further detected PAX6 following ectodermal differentiation, Desmin following mesodermal differentiation, and SOX17 following endodermal differentiation (Fig. 3B). Together, these findings support the capacity of the SD patient- and control-derived iPSC lines to generate derivatives of all three embryonic germ layers.

All iPSC lines have been submitted to the Human Pluripotent Stem Cell Registry (hPSCreg); registration is pending confirmation.

Differentiation of SD Patient- and Control-Derived iPSCs into iMSCs

Patient- and healthy-control-derived iPSCs were differentiated into iMSCs as an intermediate step before chondrogenic differentiation (Fig. 4A). During the first week of passage 0, morphological changes became apparent between days 4 and 7. The cells gradually lost their compact iPSC colony appearance and developed an elongated, spindle-shaped, fibroblast-like morphology consistent with a mesenchymal-like phenotype (Fig. 4B). Immunofluorescence staining was performed for the mesenchymal surface markers CD90 and CD105 (Fig. 4C). RT-qPCR was also performed to assess the expression of the mesenchymal marker *CD73* and the transcription factor *RUNX1* in the differentiated iMSC populations (Fig. 4D). Relative *CD73* expression in KAIMRCi009-B-derived-iMSC was two to three orders of magnitude lower than in the other three lines (Fig. 4D). These values may indicate clone-to-clone variability in the efficiency of mesenchymal marker induction.

Chondrogenic Differentiation of SD Patient- and Control-Derived iMSCs

Patient- and healthy-control-derived iMSC-like cells were cultured as three-dimensional pellets for 21 days to assess their chondrogenic differentiation potential (Fig. 5A). At the end of the culture period, control-derived cultures formed compact, rounded pellets, whereas patient-derived cultures appeared less compact and more dispersed in the tubes (black arrows; Fig. 5B). Whole-pellet Alcian Blue staining was observed in the control-derived pellets, and fainter staining was observed in the dispersed patient-derived material (Fig. 5C).

Discussion

COL2A1-associated skeletal dysplasias are predominantly inherited in an autosomal dominant manner, studying affected patients from the Saudi population remains important for understanding the genetic diversity of these disorders[2]. The burden of inherited diseases also highlights the importance of genetic diagnosis and developing patient-specific models to investigate rare genetic conditions [4, 16].

Patient-derived induced pluripotent stem cells (iPSCs) offer an approach for studying genetic disorders, particularly when affected tissues are difficult to obtain. This is relevant to type II collagenopathies, as

cartilage tissue and viable chondrocytes are not readily accessible from patients [4, 17]. In this study, we generated iPSC lines from a patient with skeletal dysplasia carrying the heterozygous *COL2A1* variant p.(Gly621Arg) and his unaffected mother as a related, non-isogenic control. PBMCs were reprogrammed using non-integrating episomal vectors, following an approach similar to that described by Alowaysi et al. [18]. Two independent iPSC clones were established from each donor, and all four lines showed typical pluripotent stem cell morphology.

The generated iPSC lines were characterized to confirm their identity, genomic stability, and pluripotency. Both patient- and control-derived lines showed normal karyotypes, STR profiles matching their respective donors, clearance of episomal vectors by (p10-13), and negative mycoplasma results. The lines also expressed the pluripotency markers OCT4, SOX2, and NANOG and demonstrated differentiation potential toward all three germ layers. Reduced OCT4 and NANOG expression following differentiation further supported their transition away from the pluripotent state. These findings are consistent with established iPSC characterization criteria and previous reports [18, 19].

To investigate their chondrogenic potential, the iPSCs were first differentiated into induced mesenchymal stem cells (iMSCs) following the protocol described by Khan et al. [7]. During differentiation, the cells acquired an elongated, spindle-shaped morphology and expressed the mesenchymal-associated markers *RUNX1* and *CD73*. Similar morphological and molecular characteristics have been reported in previous iMSC studies [7]. These findings supported the generation of iMSC-like populations from both patient- and control-derived iPSCs.

Although, following chondrogenic differentiation, patient- and control-derived iMSC-like cells exhibited observable differences in pellet morphology and Alcian Blue staining, which indicate the presence of a glycosaminoglycan-rich extracellular matrix [7, 20], these qualitative observations do not prove impaired chondrogenesis or reduced extracellular matrix production in patient-derived cells. Notably, KAIMRCi009-B-derived-iMSC showed the lowest *CD73* transcript level of the four lines yet formed a compact, strongly Alcian Blue-positive pellet, indicating that *CD73* transcript abundance did not directly predict chondrogenic pellet formation in this dataset. Because of the limited material recovered from the patient-derived pellets, chondrogenic marker expression could not be analyzed. Further quantitative experiments and comparison with isogenic controls would be required to determine whether these differences are directly associated with the *COL2A1* variant.

Previous studies have established iPSC models carrying different *COL2A1* variants, including p.(Arg989Cys), p.(Gly1113Cys), and p.(Arg719Cys), using CRISPR/Cas9 gene editing[8–10]. These models have helped investigate abnormalities in collagen processing and cartilage matrix formation. Okada et al. reported intracellular accumulation of type II collagen, endoplasmic reticulum distension, and reduced cartilage matrix formation in patient-derived models [4]. Similarly, studies involving the p.(Gly1170Ser) and p.(Arg719Cys) variants showed abnormalities in procollagen II processing and extracellular matrix organization [3, 11]. However, among the studies reviewed, no patient-derived iPSC model carrying the p.(Gly621Arg) variant was identified. In the present study, we established patient-derived iPSC lines

carrying this variant, providing a model for investigating its effects on cartilage development within the patient's genetic background. Although a healthy related control was included, further studies are needed to determine whether the observed differences in chondrogenic differentiation are directly associated with the variant.

In conclusion, we successfully established and characterized patient-derived iPSC lines carrying the heterozygous *COL2A1* p.(Gly621Arg) variant, along with lines from an unaffected, related (non-isogenic) control. Both groups demonstrated pluripotency and the ability to differentiate into iMSC-like cells. These genetically characterized lines provide a resource for future studies of *COL2A1*-associated skeletal dysplasia, including quantitative chondrogenic analyses with isogenic controls.

Table 1
List of antibodies and primers used in this study

Antibodies used for Immunofluorescence/flow-cytometry			
	Antibody	**Dilution**	**Company Cat #**
Pluripotency Markers	OCT4 Polyclonal Antibody	1:200	Thermofisher Cat# PA5-27438 RRID# AB_2544914
	Nanog Monoclonal Antibody	1:200	Thermofisher Cat# MA5-32198 RRID# AB_2809485
	SOX2 Monoclonal Antibody	1:200	Thermofisher Cat# MA1-014 RRID# AB_2536667
Differentiation markers	Rabbit anti-Desmin	1:50	Thermofisher Cat# MA5-32068 RRID# AB_2809362
	Mouse anti-SOX17	1:50	Thermofisher Cat# MA5-24885 RRID# AB_2725396
	Mouse anti-PAX6	1:50	Thermofisher Cat# MA1-109 RRID# AB_2536820
iMSC differentiation markers	Mouse anti-CD105, clone MEM-229	1:50	Antibodies.com Cat# A85494 RRID# AB_2752921
	Mouse anti-CD90/Thy-1, clone 5E10	1:50	Antibodies.com Cat# A86415 RRID# AB_2753041
Secondary antibody	Goat anti-Rabbit Secondary Antibody, Alexa Fluor 488	IF 1:200 Flow Cyt 1:2000	Abcam Cat#: ab150077 RRID# AB_2630356
	Goat anti-Mouse Secondary Antibody	IF 1:200 Flow Cyt 1:2000	Thermo Fisher Scientific Cat# 35502 RRID: AB_844397
Primers and Oligonucleotides used in this study			
	Target	Forward/Reverse primer (5'-3')	
Pluripotency RT-qPCR Primers	*OCT4*	Forward: CTGGGTTGATCCTCGGACCT Reverse: CCATCGGAGTTGCTCTCCA	

Antibodies used for Immunofluorescence/flow-cytometry		
	Antibody	**Dilution Company Cat #**
	NANOG	Forward: TTTGTGGGCCTGAAGAAAACT
		Reverse: AGGGCTGTCCTGAATAAGCAG
	SOX2	Forward: GCCGAGTGGAAACTTTTGTCG
		Reverse: GGCAGCGTGTACTTATCCTTCT
Differentiation RT-qPCR Primers	*BRACHYURY or TBXT*	Forward: TAAGGTGGATCTTCAGGTAGC
		Reverse: CATCTCATTGGTGAGCTCCCT
	CDX2	Forward: GACGTGAGCATGTACCCTAGC
		Reverse: GCGTAGCCATTCCAGTCCT
	NESTIN	Forward: CTGCTACCCTTGAGACACCTG
		Reverse: GGGCTCTGATCTCTGCATCTAC
	PAX6	Forward: TGGGCAGGTATTACGAGACTG
		Reverse: ACTCCCGCTTATACTGGGCTA
	SOX17	Forward: GCATTCTGGAATGAGCCTACT
		Reverse: GGGCAGGTCAAGCTTATGAT
	GATA4	Forward: CGACACCCCAATCTCGATATG
		Reverse: GTTGCACAGATAGTGACCCGT
IMSCs Differentiation RT-qPCR Primers	*RUNX1*	Forward: AACCTCAGCCTCAGAGTCA
		Reverse: CAATGATCCCAGGTATTGG
	CD73	Forward: CAGCGAGGACTCCAGCAAG
		Reverse: TATCCAACGATTCCCACAACT
House-Keeping Genes RT-qPCR Primers	*GAPDH*	Forward: GGAGCGAGATCCCTCCAAAAT
		Reverse: GGCTGTTGTCATACTTCTCATGG
Mutation analysis Primers	*COL2A1*	Forward: CTT GGC TGT CCA TCA GGA TGT G
		Reverse: AAG CCG AAG TGA CAA GCG TTA G
Sanger analysis primer	*COL2A1*	CTT GGC TGT CCA TCA GGA TGT G
EBNA-1 Primers	pEP4-SF2-oriP	Forward: ATC GTC AAA GCT GCA CAC AG
	pEP4-SR2-oriP	Reverse: CCC AGG AGT CCC AGT AGT CA

Declarations

Conflict of interest

the authors declare that they have no conflict of interest.

Declarations of AI use

The authors declare the use of an AI-based large language model tool to improve the readability, grammar, and language of the manuscript. The authors reviewed and edited the content as needed and take full responsibility for the content of the publication.

Ethical approval

This study was approved by the Institutional Review Board of King Abdullah International Medical Research Center (KAIMRC) (Protocol No. NRJ22J/060/03).

Informed consent

Written informed consent was obtained from the patient's legal guardian and from the control donor.

Funding

This study was funded by King Abdullah International Medical Research Center (KAIMRC).

Author contributions

K.A. developed the study concept, obtained funding, supervised the project, and prepared the manuscript. M.H. contributed to the study design, supervised the experimental work, performed experiments and STR analysis, analyzed the data, prepared figures, and wrote the manuscript. L.A. assisted with donor and patient recruitment, conducted experiments, analyzed data, prepared figures, and supported the informed consent process. M.B., G.R., and M.A.-S. performed experiments. M.A.B. conducted and analyzed the flow cytometry experiments. M.D., H.H., R.A.J., H.A., L.B., D.A., and S.A.K. performed and analyzed the karyotyping studies. D.A.-Y. and A.E. provided scientific guidance, supervision, and consultation. All authors reviewed and approved the final manuscript.

Acknowledgements

We thank Pfizer Ireland Pharmaceuticals for supporting the establishment of the Saudi Bank of Human iPSCs. We also acknowledge the continued support of the Local Content and Government Procurement

Authority (LCGPA) in Saudi Arabia. We are grateful to the donor and his family for their contribution to scientific research.

Data availability

The data supporting the findings of this study are available from the corresponding author upon reasonable request. Requests for access to this data should be directed to Dr. Khaled Alsayegh, alsayeghk@kaimrc.med.sa.

References

1. Cho SY, Jin D-K. Guidelines for genetic skeletal dysplasias for pediatricians. Ann Pediatr Endocrinol Metab. 2015;20:187. https://doi.org/10.6065/apem.2015.20.4.187.
2. Deng H, Huang X, Yuan L. Molecular genetics of the COL2A1-related disorders. Mutat Research/Reviews Mutat Res. 2016;768:1–13. https://doi.org/10.1016/j.mrrev.2016.02.003.
3. Yammine KM, Mirda Abularach S, Kim S, Bikovtseva AA, Lilianty J, Butty VL, et al. ER procollagen storage defect without coupled unfolded protein response drives precocious arthritis. Life Sci Alliance. 2024;7:e202402842. https://doi.org/10.26508/lsa.202402842.
4. Okada M, Ikegawa S, Morioka M, Yamashita A, Saito A, Sawai H, et al. Modeling type II collagenopathy skeletal dysplasia by directed conversion and induced pluripotent stem cells. Hum Mol Genet. 2015;24:299–313. https://doi.org/10.1093/hmg/ddu444.
5. Wu Z, Korntner S, Mullen A, Zeugolis D. Collagen type II: From biosynthesis to advanced biomaterials for cartilage engineering. Biomaterials Biosystems. 2021;4:100030. https://doi.org/10.1016/j.bbiosy.2021.100030.
6. Liang G, Lian C, Huang D, Gao W, Liang A, Peng Y, et al. Endoplasmic Reticulum Stress-Unfolding Protein Response-Apoptosis Cascade Causes Chondrodysplasia in a col2a1 p.Gly1170Ser Mutated Mouse Model. PLoS ONE. 2014;9:e86894. https://doi.org/10.1371/journal.pone.0086894.
7. Khan N, Diaz-Hernandez M, Drissi H. Differentiation of Human Induced Pluripotent Stem Cells (iPSCs)–derived Mesenchymal Progenitors into Chondrocytes. Bio Protoc 2023;13. https://doi.org/10.21769/BioProtoc.4874
8. Lilianty J, Nur Patria Y, Stanley EG, Elefanty AG, Bateman JF, Lamandé SR. Generation of a heterozygous COL2A1 (p.R989C) spondyloepiphyseal dysplasia congenita mutation iPSC line, MCRIi001-B, using CRISPR/Cas9 gene editing. Stem Cell Res. 2020;45:101843. https://doi.org/10.1016/j.scr.2020.101843.
9. Lilianty J, Bateman JF, Lamandé SR. Generation of a heterozygous COL2A1 (p.G1113C) hypochondrogenesis mutation iPSC line, MCRIi019-A-7, using CRISPR/Cas9 gene editing. Stem Cell Res. 2021;56:102515. https://doi.org/10.1016/j.scr.2021.102515.

10. Yammine KM, Mirda Abularach S, Sampurno L, Bateman JF, Lamandé SR, Shoulders MD. Using CRISPR/Cas9 to generate a heterozygous COL2A1 p.R719C iPSC line (MCRIi019-A-6) model of human precocious osteoarthritis. Stem Cell Res. 2023;67:103020. https://doi.org/10.1016/j.scr.2023.103020.
11. Yammine KM, Mirda Abularach S, Xiong M, Kim S, Bikovtseva AA, Butty VL, et al. Failed cellular surveillance enables pathogenic matrix deposition in a COL2A1-related osteoarthritis. J Biol Chem. 2025;301:110436. https://doi.org/10.1016/j.jbc.2025.110436.
12. Shoulders MD, Raines RT. Collagen Structure and Stability. Annu Rev Biochem. 2009;78:929–58. https://doi.org/10.1146/annurev.biochem.77.032207.120833.
13. Long CG, Braswell E, Zhu D, Apigo J, Baum J, Brodsky B. Characterization of Collagen-like Peptides Containing Interruptions in the Repeating Gly-X-Y Sequence?32. 1993.
14. Bella J, Eaton M, Brodsky B, Berman HM. Crystal and Molecular Structure of a Collagen-Like Peptide at 1.9 Å Resolution. Science (1979) 1994;266:75–81. https://doi.org/10.1126/science.7695699
15. National Center for Biotechnology Information. NM_001844.5(COL2A1):c.1861G > A (p.Gly621Arg) 2026. https://www.ncbi.nlm.nih.gov/clinvar/variation/196112/(accessed October 15, 2026).
16. Alqahtani AS, Alotibi RS, Aloraini T, Almsned F, Alassali Y, Alfares A, et al. Prospect of genetic disorders in Saudi Arabia. Front Genet. 2023;14. https://doi.org/10.3389/fgene.2023.1243518.
17. Volpato V, Webber C. Addressing variability in iPSC-derived models of human disease: guidelines to promote reproducibility. Dis Model Mech. 2020;13. https://doi.org/10.1242/dmm.042317.
18. Alowaysi M, Lehmann R, Al-Shehri M, Baadhaim M, Alzahrani H, Aboalola D, et al. HLA-based banking of induced pluripotent stem cells in Saudi Arabia. Stem Cell Res Ther. 2023;14:374. https://doi.org/10.1186/s13287-023-03612-0.
19. Sullivan S, Stacey GN, Akazawa C, Aoyama N, Baptista R, Bedford P, et al. Quality Control Guidelines for Clinical-Grade Human Induced Pluripotent Stem Cell Lines. Regenerative Med. 2018;13:859–66. https://doi.org/10.2217/rme-2018-0095.
20. Whiteman P. The quantitative measurement of Alcian Blue–glycosaminoglycan complexes. Biochem J. 1973;131:343–50. https://doi.org/10.1042/bj1310343.

Figures

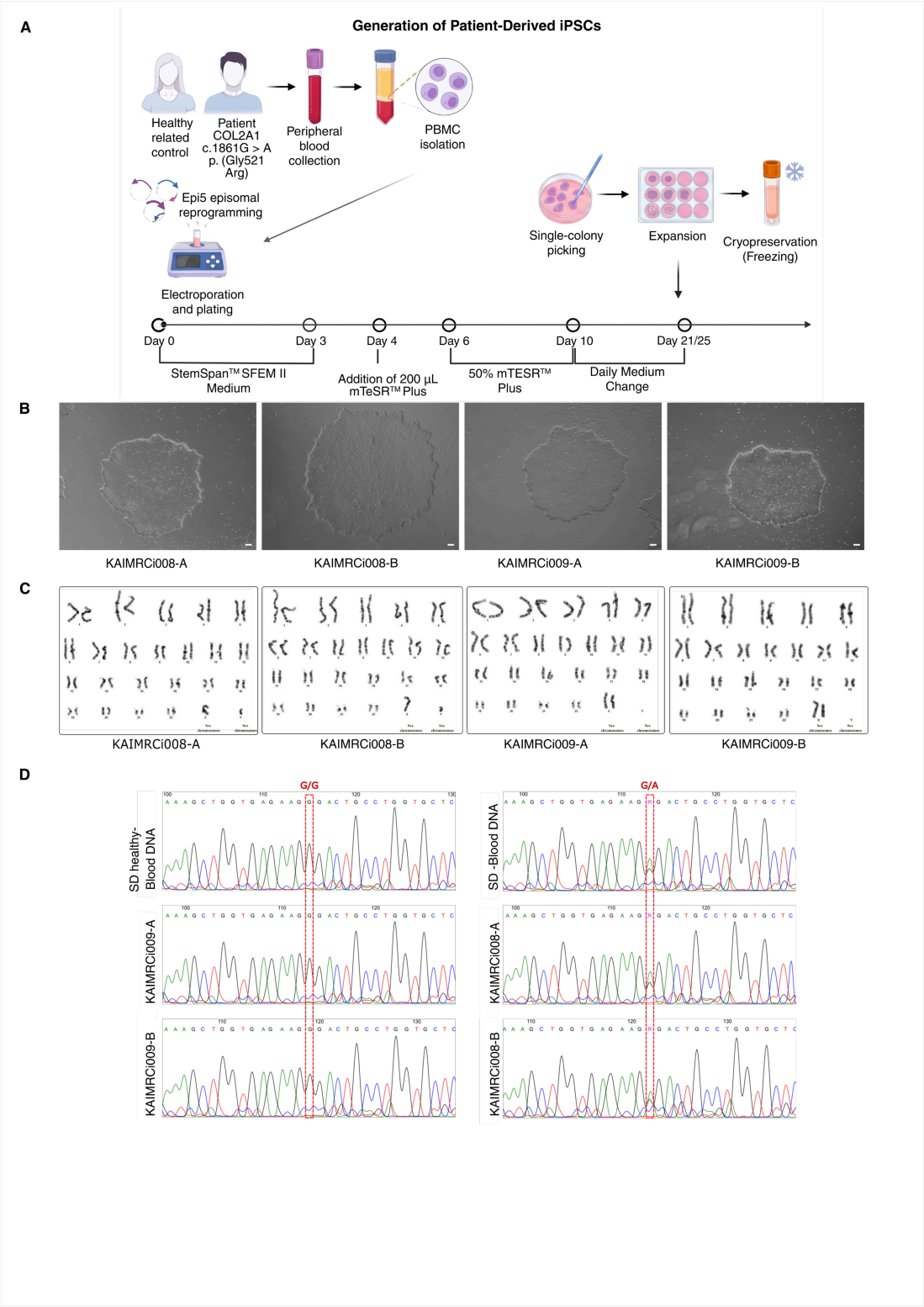

Figure 1

Generation and initial characterization of patient- and control SD- iPSC lines. (A) A diagram illustrates PBMCs reprogramming and iPSC colonies establishment using a non-integrating episomal system. Schematic illustrations were created with BioRender.com. (B) Representative phase-contrast images of colonies from SD-iPSC lines and two related-control lines exhibiting standard iPSC morphology with high nucleus-to-cytoplasm ratio and defined borders. Scale bar, 100 µm. (C) Representative G-banded

karyotypes analysis showing 46, XY for patient-derived iPSC lines and 46, XX for healthy related-control-derived iPSC lines. (D) Sanger sequencing chromatograms of the patient and corresponding healthy related control samples, showing the heterozygous *COL2A1*NM_001844.5: c.1861G>A, p.(Gly621Arg) variant in the patient samples and the corresponding PBMCs.

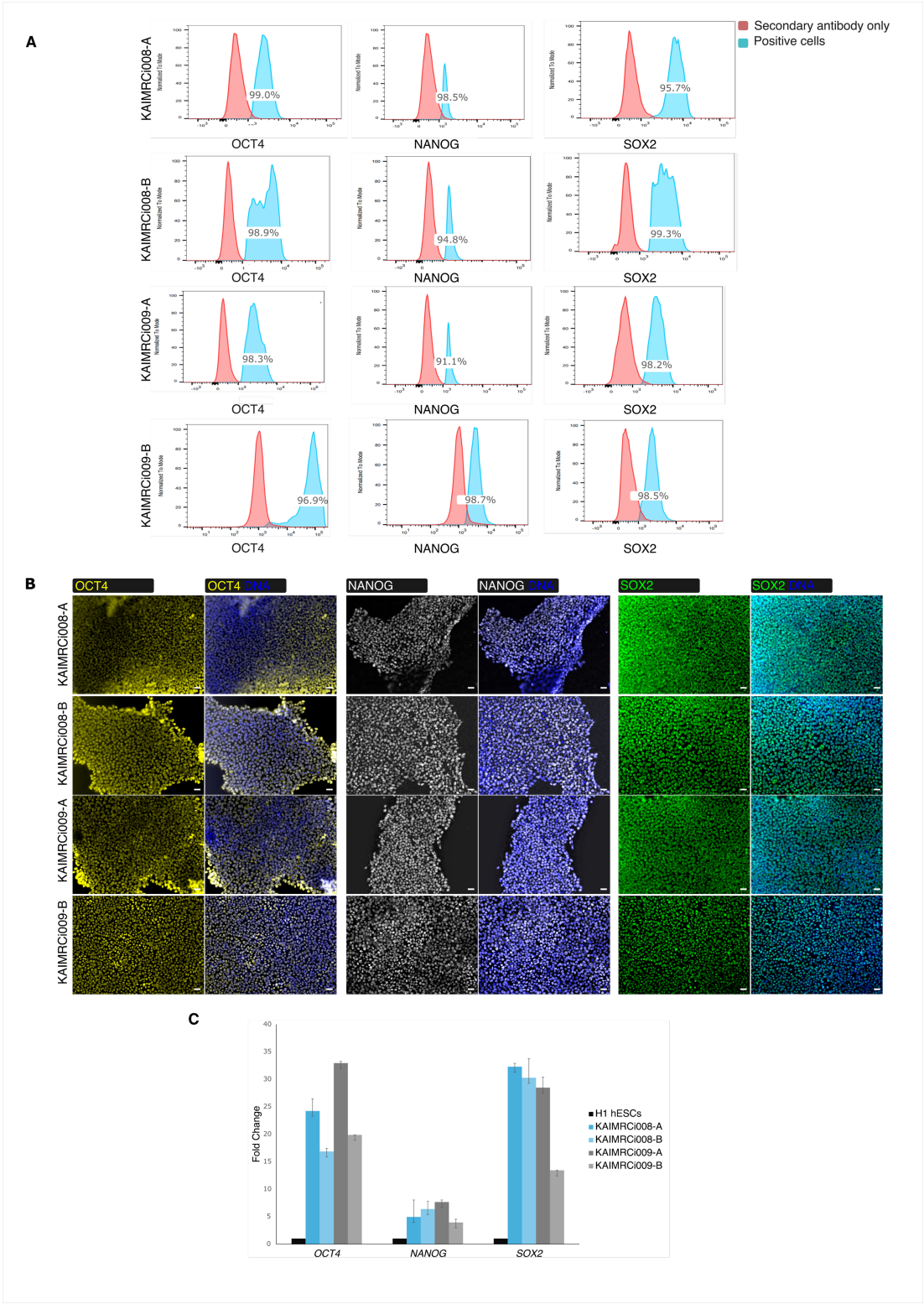

Figure 2

Pluripotency characterization of patient- and control SD- iPSC lines. (A) Flow-cytometry analysis of OCT4, SOX2, and NANOG expression in patient- and healthy related-control-derived iPSC clones. Red histograms, secondary antibody-only control; blue histograms, stained cells (B) Immunofluorescence staining for OCT4 (yellow), SOX2 (green), and NANOG (white) in patient- and healthy related-control-derived iPSC clones. Nuclei were stained with DAPI (blue). Scale bar = 100 μm. (C) RT-qPCR analysis of *OCT4*, *SOX2*, and *NANOG* expression in the established iPSC clones, the data was normalized to *GAPDH* and expressed as fold change (2^−ΔΔCt) relative to H1 hESCs. Data were obtained from three biological replicates, with each sample analyzed in technical triplicates. Results are presented as mean ± SD.

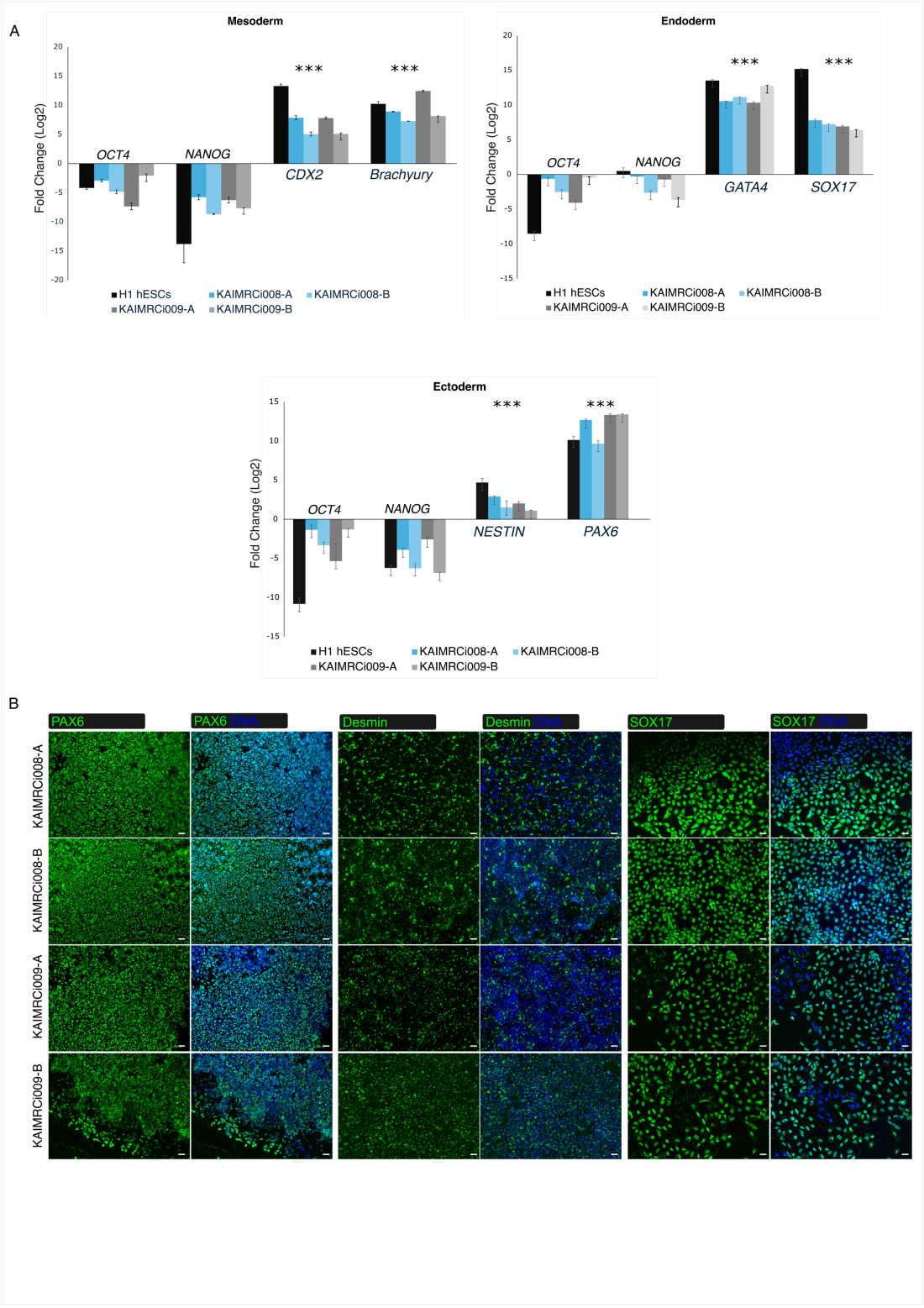

Figure 3

Trilineage differentiation of patient- and control SD- iPSC lines. (A) RT-qPCR analysis of ectodermal (*PAX6* and *NESTIN*), mesodermal (*TBXT* and *CDX2*), and endodermal (*SOX17* and *GATA4*) markers expression after directed differentiation. Data was normalized to *GAPDH* and expressed as log2 fold change relative to the corresponding undifferentiated iPSCs; H1 hESCs were differentiated in parallel as a reference. Data were obtained from three biological replicates, with each sample analyzed in technical

triplicates. Results are presented as mean ± SD. Statistical significance was assessed using an unpaired two-tailed Student's t-test, ***p < 0.001 versus the corresponding undifferentiated iPSCs. (B) Immunofluorescence staining showing successful differentiation into the three germ layers: ectoderm (PAX6, green), mesoderm (DESMIN, green), and endoderm (SOX17, green). Nuclei were stained with DAPI (blue). Scale bar = 100 µm.

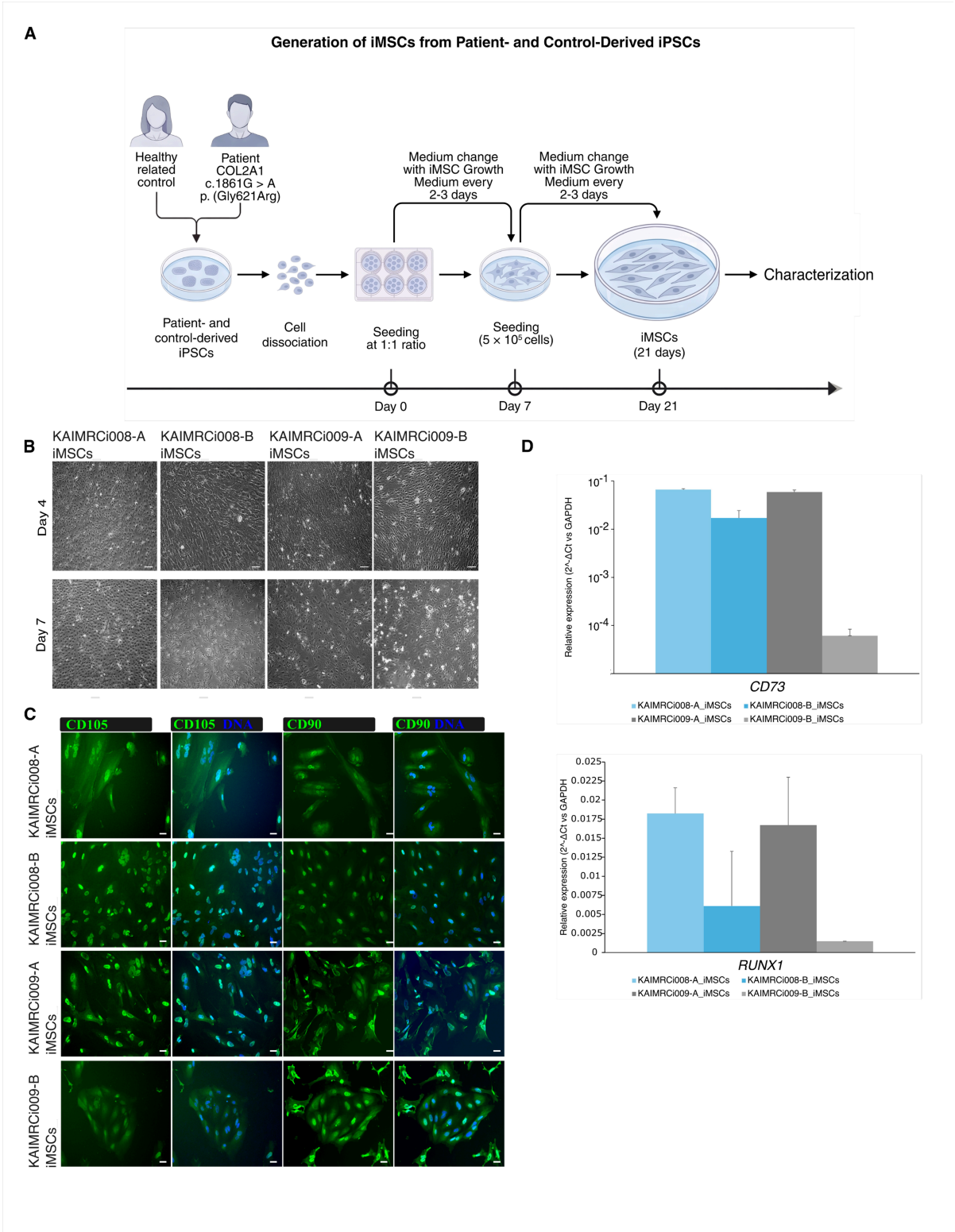

Figure 4

Differentiation and characterization of iPSC-derived mesenchymal stem cells. (A). A diagram illustrating the generation of iMSCs from patient- and control SD- iPSC lines. Schematic illustrations were created with BioRender.com. (B) Representative phase-contrast images of patient- and healthy related-control-derived cultures at day 4 and 7 of iMSC-like phenotype differentiation, showing progressive development of a spindle-shaped, mesenchymal-like morphology. Scale bar = 100 µm. (C) Immunofluorescence staining for CD90 (green) and CD105 (green) in patient- and healthy related-control-derived iMSC-like cells. Nuclei were stained with DAPI (blue). Scale bar = 100 µm. (D) RT-qPCR analysis of *RUNX1* and *CD73*expression in patient- and healthy related-control-derived iMSC-like cells. Data are relative expression (2^−ΔCt) normalized to *GAPDH*. Data were obtained from three technical replicates. Results are presented as mean ± SD.

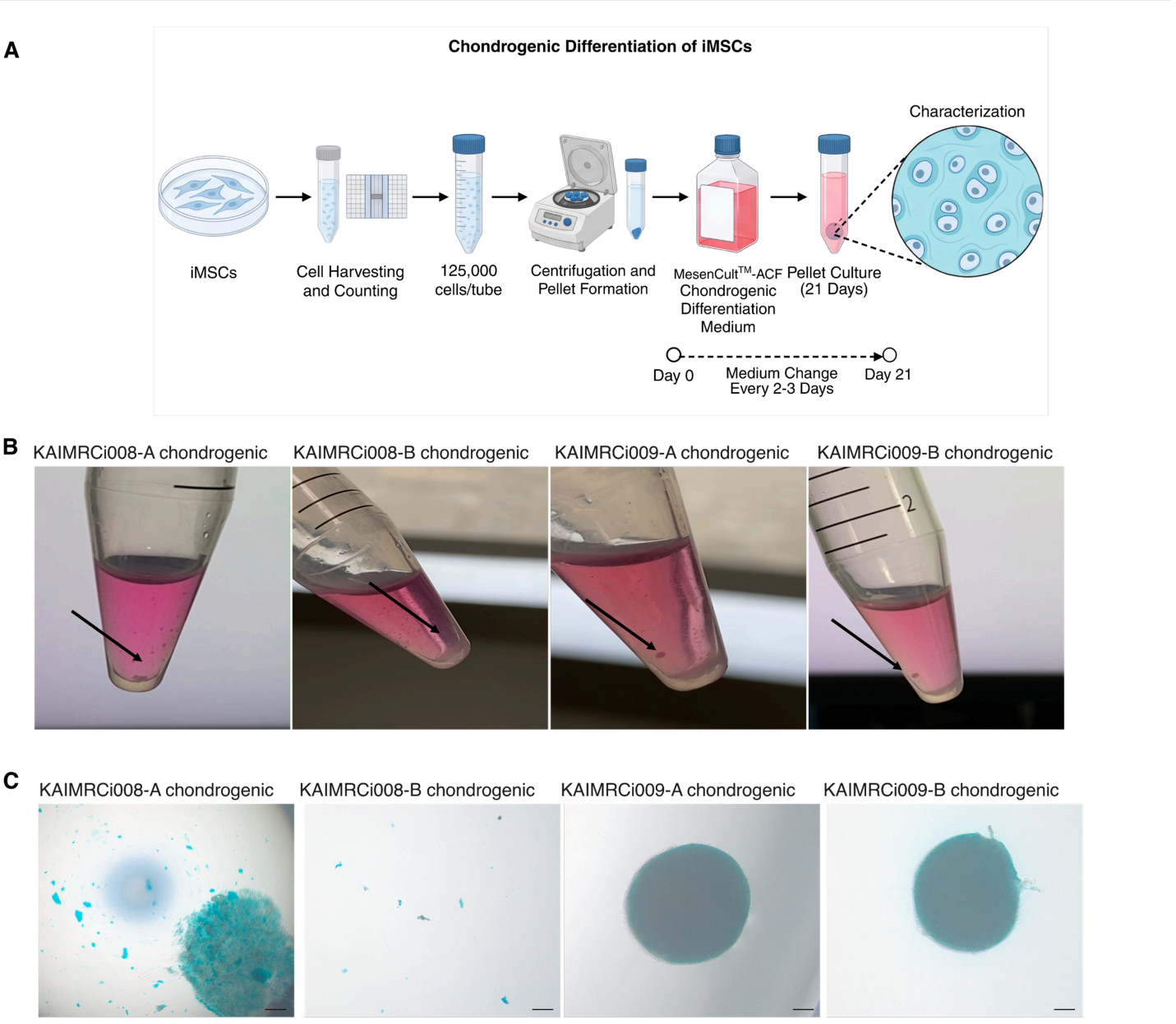

Figure 5

Chondrogenic differentiation of patient- and healthy-derived SD-iMSCs. (A) Schematic of the 21-day three-dimensional pellet culture workflow for chondrogenic differentiation. Schematic illustrations were created with BioRender.com. (B) Representative images of healthy and patient-derived chondrogenic pellets in 15-mL conical tubes at the end of differentiation. Healthy-derived chondrogenic pellets appeared compact and rounded (black arrow), whereas patient-derived pellets appeared less compact and dispersed (black arrow). One pellet was formed per tube, and four pellets per line were generated. (C) Representative images of Alcian Blue-stained chondrogenic pellets from healthy-control- and patient-derived cultures following chondrogenic differentiation. Scale bar = 100 μm.

Supplementary Files

This is a list of supplementary files associated with this preprint. Click to download.

- S11.png